Transactions of the Materials Research Society of Japan 29[7] 3033-3036 (2004)

Relation between Composition and Shape Memory Effect of the Sputtered Films of Ferromagnetic Shape Memory Alloy Ni_2MnGa

Yuya Konno[*+], Makoto Ohtsuka[**,++], Minoru Matsumoto[**] and Kimio Itagaki[**]
[*]Graduate Student, Tohoku University, Sendai 980-8577, JAPAN
Fax: 81-22-217-5211, [+]e-mail: ykonno@mail.tagen.tohoku.ac.jp
[**]IMRAM, Tohoku University, Sendai 980-8577, JAPAN
Fax: 81-22-217-5211, [++]e-mail: ohtsuka@tagen.tohoku.ac.jp

Shape memory effect by the magnetic field is interesting and important for physics and application. The sputtered films of ferromagnetic shape memory alloy Ni_2MnGa were prepared by a radio-frequency magnetron sputtering apparatus using three kinds of Ni-Mn-Ga targets. The composition of Ni_2MnGa sputtered films was controlled by the sputtering power and composition of target. The obtained films were heat-treated at 1073 K for 3.6 ks for homogenization and atomic ordering, and then cooled in a furnace. They were constrained in a silica tube and heated to make the shape memory effect. The composition of films was determined by inductively coupled plasma mass spectrometry (ICP). Transformation temperatures were found to be dependent on the composition of films. The film was set into a thermostatic bath in which the temperature was precisely controlled. The shape change of films was recorded by a video camera. The constrain-aged films showed a two-way shape memory effect by heating and cooling. The effect of composition on the shape memory effect is discussed.

Key words: two-way shape memory effect, sputtered film, ferromagnetic shape memory alloy, martensitic transformation, constraint-aging

1. INTRODUCTION

The ternary Ni_2MnGa alloy has a ferromagnetic property and a shape memory effect. It has the Heusler type crystal structure at high temperature and some martensitic crystal structures at low temperature [1-4]. The martensitic transformation of stoichiometric and non-stoichiometric composition Ni_2MnGa occurs in the ferromagnetic region below Curie temperature and can be controlled not only by temperature and stress but also by magnetic field [5]. However, the Ni_2MnGa bulk alloy is too brittle to be formed in a required shape. Furthermore, it has a disadvantage of very slow response to the shape memory effect by temperature change.

To solve these problems, the use of the Ni_2MnGa alloy films prepared by the sputtering method has been proposed by the authors [6-8]. It may be applied for an actuator of micro-machines. In order to use this actuator at around room temperature, martensitic transformation and the Curie temperature should be higher than room temperature. It was found that the heat-treated Ni-rich Ni_2MnGa alloy films will satisfy this requirement. Martensitic transformation temperature increased and Curie temperature slightly decreased with increasing nickel content of $Ni_{2+x}Mn_{1-x}Ga$ bulk alloy (x = 0 ~ 0.19) [9]. The chemical composition of film depends on that of the target and sputtering electric power [6]. Two-way shape memory effect by heating and cooling was found to be induced by the plastic deformation [7] and the constraint-aging method [8]. Using the two-way shape memory effect, miniaturization and simplification of a device will be made possible. Furthermore, the shape memory effect of the constraint-aged Ni_2MnGa films by magnetic field was also observed [10].

In the present study, the relation between the composition and shape memory effect of the aged Ni_2MnGa films prepared by the constraint-aging method has been investigated.

2. EXPERIMENTAL PROCEDURE

2.1 Preparation of films

The Ni-rich Ni_2MnGa films were deposited on a poly-vinyl alcohol (PVA) substrate with a radio-frequency (RF) magnetron sputtering apparatus (Shibaura, CFS-4ES) using three kinds of $Ni_{52.5}Mn_{22}Ga_{25.5}$, $Ni_{54}Mn_{20}Ga_{26}$ and $Ni_{55}Mn_{18}Ga_{27}$ targets. The sputtering conditions were as follows: base pressure, $< 2.5 \times 10^{-4}$ Pa; argon working-gas pressure, 6×10^{-1} Pa; substrate temperature, 323 K; sputtering power, 200 W. The thickness of the deposited films was kept about 5 μm by controlling the sputtering time. After the deposition, the films were separated from the PVA substrate by using hot water and then films were heat-treated at 1073 K for 3.6 ks for homogenization and atomic ordering, and cooled in a furnace.

After the heat-treatment, the films were cut into 5 mm × 12 mm, deformed to a cylindrical shape, and then fixed inside a silica tube whose inner diameter was 4 mm. These constraint films were aged at 673 K for 3.6

ks in a flow of argon gas, then, rapidly cooled in air. The composition of the films was determined by an inductively coupled plasma (ICP) spectrometry (Seiko, SPS-1200A). The structure of the films was measured by an X-ray diffractometer (XRD) (Rigaku, RINT2200).

2.2 Measurement of shape memory effect

The constraint-aged film was set into a thermostatic bath in which temperature was controlled. The shape memory behavior of the films was observed using a digital video camera (Sony, DCR-PC120). The measurement was performed in a temperature range between 295 and 360 K.

3. RESULTS AND DISCUSSION

3.1 Composition of films

The composition and valance electron density of as-sputtered films were shown in **Table 1**. The

Table 1 Target composition, sputtering power, film composition and valence electron density.

Sample	Composition of target	Sputtering power (W_S)	Composition of film	Valence electron density (e/a)
N54(HT)	$Ni_{52.5}Mn_{22}Ga_{25.5}$		$Ni_{54.4}Mn_{21.3}Ga_{24.3}$	7.66
N55(HT)	$Ni_{54}Mn_{20}Ga_{26}$	200W	$Ni_{55.2}Mn_{20.6}Ga_{24.2}$	7.69
N56(HT)	$Ni_{55}Mn_{18}Ga_{27}$		$Ni_{56.6}Mn_{18.5}Ga_{24.9}$	7.70

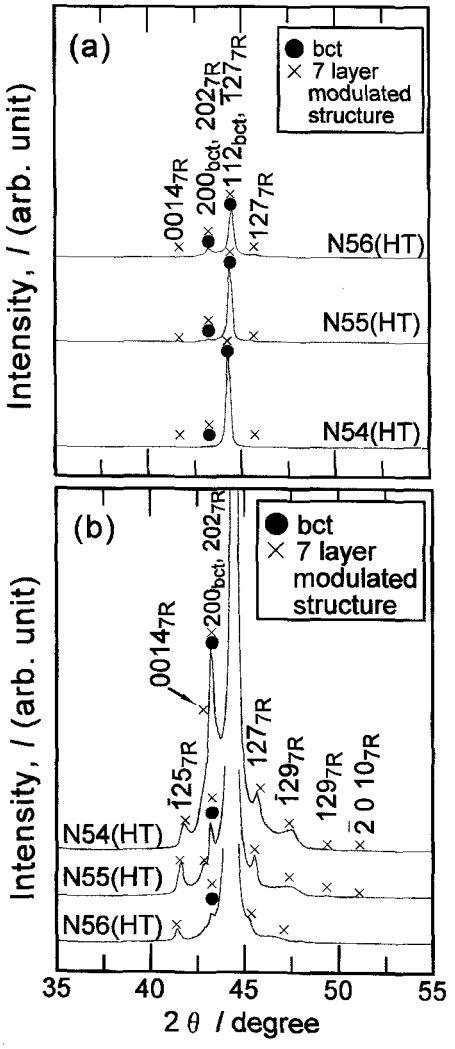

Fig. 1 X-ray diffraction patterns of N54(HT), N55(HT) and N56(HT). (b) enlarged intensity of the diffraction patterns in (a).

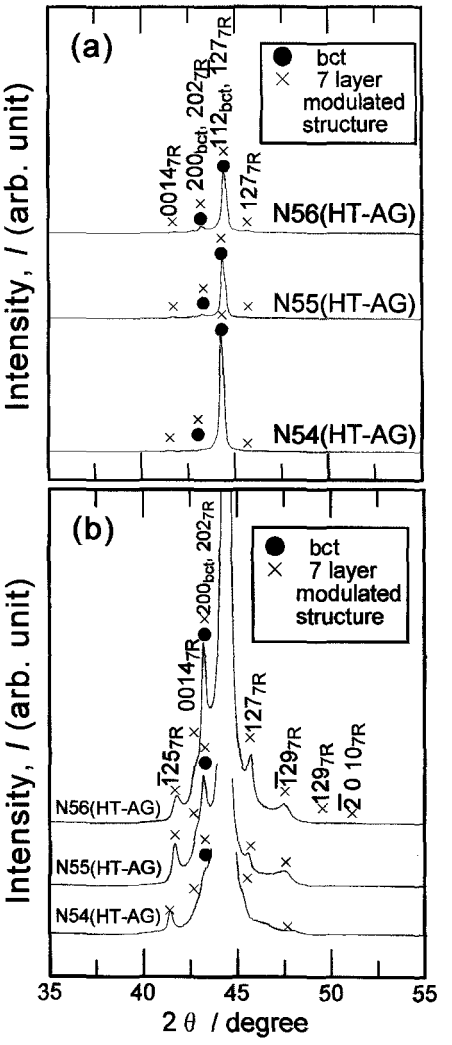

Fig. 2 X-ray diffraction patterns of N54(HT-AG), N55(HT-AG) and N56(HT-AG). (b) enlarged intensity of the diffraction patterns in (a).

composition of films was controlled by that of target and the sputtering power. Hereafter, the heat treated $Ni_{54.4}Mn_{21.3}Ga_{24.3}$ film is called as N54(HT). Similarly, others are called as N55(HT) and N56(HT). The range of valence electron density is from 7.66 to 7.70. Furthermore, $Ni_{54.4}Mn_{21.3}Ga_{24.3}$ film constrained at 673 K for 3.6 ks is called as N54(HT-AG). Similarly, others are called as N55(HT-AG) and N56(HT-AG).

3.2. Crystal structure of films

Fig. 1(a) and (b) show X-ray diffraction patterns of N54(HT), N55(HT) and N56(HT). The diffraction patters in Fig. 1(b) is shown with an enlarged scale of the ordinate in Fig. 1(a). The diffraction peaks for all heat treated films are indexed as a martensitic structure. The pattern obtained for the martensitic phase is indexed as body centered tetragonal (bct) and 7 layer modulated structure, which are reported by Martynov [4] and Pons *et al* [2]. The $(112)_{bct}$ peak shifts to high angle with increasing nickel content, whereas $(200)_{bct}$ peaks do nott shift. It is found that the lattice constant of c-axis of martensitic bct decreases with increasing nickel content.

Fig. 2 shows X-ray diffraction patterns of N54(HT-AG), N55(HT-AG) and N56(HT-AG). The diffraction patters in Fig. 2(b) is shown with an enlarged scale of the ordinate in Fig. 2(a). All constraint-aged films show the martensitic phase, bct and 7 layers modulated structure. These structures are the same as those of the heat-treated films. $(\bar{2}\ 0\ 10)_{7R}$ peak for the constraint-aged film is decreased. The intensity of the modulated structure may be changed by constant-aging.

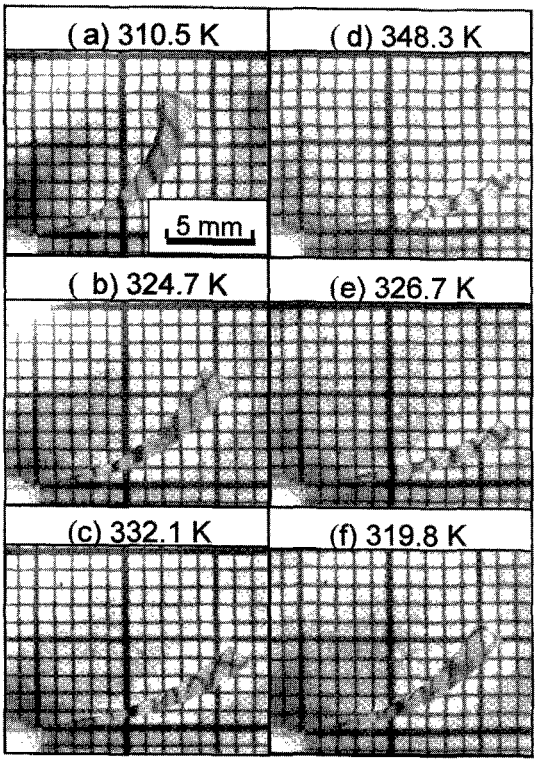

Fig. 3 Two way shape memory behavior of Ni55(HT-AG). (a)-(d) : heating, (d)-(f) : cooling.

3.3 Shape memory effect by thermal change

Fig. 3 shows the photographs of shape change of N55(HT-AG) during heating (a)-(d) and cooling (d)-(f). Heating and cooling rate was 3.3×10^{-2} K/s. One end of the film was fixed and another end was free. Temperatures in the thermostatic bath were monitored at several points and temperature distribution was almost constant.

The curvature of film increased with increasing temperature from 305 to 350 K, then it decreased with decreasing temperature from 350 to 305 K. This shape change is two-way shape memory behavior. The measurement was performed in a temperature range of martensitic and reverse martensitic transformation. From this observation, the strain $\varepsilon = (d_S/2) / r_T$, where d_S is thickness of film and r_T is radius of curvature, accompanied by the shape memory effect of the N54(HT-AG), N55(HT-AG) and N56(HT-AG) was calculated and is shown in **Fig. 4**. The symbols of (a)-(f) in Fig. 4 correspond to the photographs of (a)-(f) in Fig. 3. Strain vs. temperature curves present a similar behavior during heating and cooling. The amount of strain accompanied by the shape

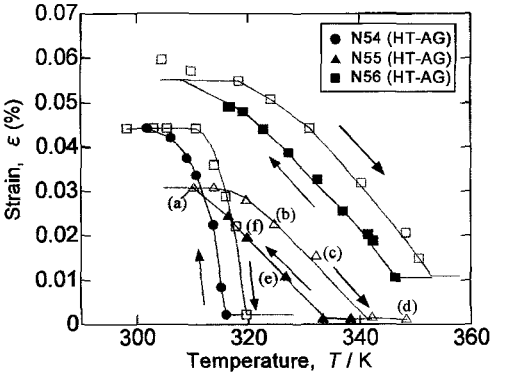

Fig. 4 Strain accompanied by two way shape memory effect of N54(HT-AG), N55(HT-AG) and N56(HT-AG).

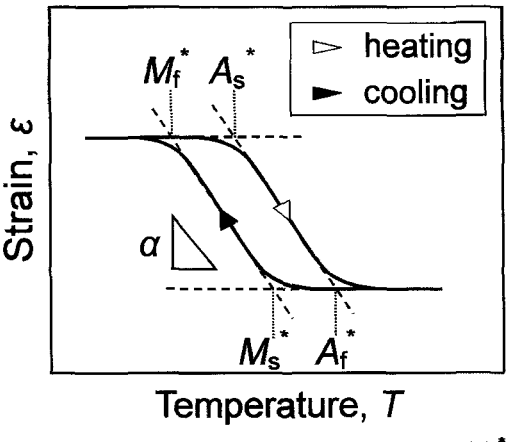

Fig. 5 Definition of various temperatures (A_s^*, A_f^*, M_s^* and M_f^*) in the strain vs. temperature curve.

Table 2 Transformation temperatures, strain of TWME, gradient and hysteresis of various constraint-aged films.

Sample	A_s^* / K	A_f^* / K	M_s^* / K	M_f^* / K	α	ε_{TWME} (%)	hysteresis / K
N54(HT-AG3.6)	314	320	316	310	6.8×10^{-5}	4.2×10^{-2}	4
N55(HT-AG3.6)	319	341	334	310	1.2×10^{-5}	2.9×10^{-2}	8
N56(HT-AG3.6)	322	355	347	314	1.4×10^{-5}	4.4×10^{-2}	8

change was different from each other in the composition at N54(HT-AG), N55(HT-AG) and N56(HT-AG). The strain was constant in the low and high temperature regions. The difference in the strain between at low temperature and high temperature was large for N54(HT-AG) and N56(HT-AG) compared to N55(HT-AG).

Fig. 5 shows a schematic strain vs. temperature curve. The inflection temperatures, A_s^*, A_f^*, M_s^* and M_f^*, were defined in the strain vs. temperature curve during heating and cooling as shown in Fig. 5. During heating, the strain in the low temperature region decreased and changed in the high temperature region. The transformation temperatures (A_s^*, A_f^*, M_s^* and M_f^*), the two way shape memory effect strain (ε_{TWME}) and the temperature hysteresis are shown in **Table 2**. ε_{TWME} is the difference between the strain at high temperature (ε_{HT}) and that at low temperature (ε_{LT}). ε_{LT} of N54(HT-AG) and N56(HT-AG) was larger than that of N55(HT-AG). The gradient, α was calculated as listed in this table. The gradient was defined as a ratio of the strain to the difference in transformation temperature, $\alpha = \varepsilon_{TWME} / (A_f^* - A_s^*)$. They indicate the magnitude of strain accompanied by the martensitic and reverse martensitic transformations per unit temperature change of 1 K. The value of N54(HT-AG) is about 5 times of the others. The hysteresis of N54(HT-AG) is about half of the others. Thus, effective two-way shape memory strain can be realized for N54(HT-AG). This film can be expected to have a magnetic-field induced shape memory effect under low magnetic field due to the large gradient and small hysteresis in the strain vs. temperature curve. The transformation temperatures of films increase with increasing nickel content. Valence electron density (e/a) increases with increasing nickel content. N55(HT-AG) and N56(HT-AG) are expected to move at higher temperature.

4. SUMARRY

1) The diffraction peaks for all the heat-treated filmscorrespond to a martensitic structure. The modulated structure may be changed by the constraint-aging.
2) The transformation temperatures increase with increasing nickel content.
3) N54(HT-AG) shows a good shape memory property, in that the gradient is large and the hysteresis is small in the strain vs. temperature curve. This film can be expected to have a magnetic-field induced shape memory effect under low magnetic field.

Acknowledgement

The research was partly supported by Industrial Technology Research Grant Program in '02 from New Energy and Industrial Technology Development Organization (NEDO) of Japan.

References

[1] P. J. Webster, K. R. A. Ziebeck, S. L. Town and M. S. Peak, *Philos. Mag. B*, **49**, 295 - 310 (1984).
[2] J. Pons, V. A. Chernenko, R. Santamarta and E. Cesari, *Acta Mater.*, **48**, 3027 - 3038 (2000).
[3] B. Wedel, M. Suzuki, Y. Murakami, C. Wedel, T. Suzuki, D. Shindo and K. Itagaki, *J. Alloys Comp.*, **290**, 137 - 143 (1999).
[4] V. V. Martynov., *J. de physiq. IV*, **5**, C8 - 91. (1995)
[5] K. Ullakko, *J. Mater. Eng. Perform.*, **5**, 405 - 409 (1996).
[6] K. Ohi, S. Isokawa, M. Ohtsuka, M. Matsumoto and K. Itagaki, *Trans. Mater. Res. Soc. Japan*, **26**, 291 - 294 (2001).
[7] M. Ohtsuka, M. Matsumoto and K. Itagaki, *Trans. Mater. Res. Soc. Japan*, **26**, 201 - 204 (2001).
[8] S. Isokawa, M. Suzuki, M. Ohtsuka, M. Matsumoto and K. Itagaki, *Mater. Trans.*, **42**, 1886 - 1889 (2001).
[9] M. Matsumoto, T. Takagi, J. Tani, T. Kanomata, N. Muramatsu and A. N. Vasil'ev, *Mater. Sci. Eng.*, **A 273 - 275**, 326 - 328 (1999).
[10] M. Sanada, M. Ohtsuka, M. Matsumoto, T. Takagi and K. Itagaki, *Trans. Mater. Res. Soc. Japan*, **28**, 663 - 666 (2003).

(Received October 10, 2003; Accepted March 20, 2004)